

## CREEP BEHAVIOUR IN A ROTATING DISC IN THE PRESENCE OF PARTICLE AND THERMAL GRADIENTS

### PUZANJE KOD ROTACIONOG DISKA U PRISUSTVU GRADIJENATA ČESTICA I TEMPERATURE

Originalni naučni rad / Original scientific paper

UDK /UDC: 539.434

Rad primljen / Paper received: 2.10.2017.

Adresa autora / Author's address:

Punjabi University, Department of Mathematics, Patiala, Punjab, India email: [vaggarwal2584@gmail.com](mailto:vaggarwal2584@gmail.com)

#### Keywords

- modelling
- creep
- functionally graded rotating disc
- composites

#### Abstract

*The creep behaviour of a rotating disc made of isotropic composite containing varying amount of SiC particles in the radial direction has been investigated in the presence of thermal gradients also in the radial direction. The thermal gradient experienced by the disc is the result of breaking action as estimated by finite element method. The creep behaviour has been described by Norton's law. The results indicate that steady state creep rates are significantly decreased in the presence of linear particle gradient and/or thermal gradients, as compared to a composite disc with the same average particle content distributed uniformly and operating under isothermal conditions.*

#### INTRODUCTION

The functionally graded material (FGM) concept originated in Japan in 1984 during the space-plane project, in the form of a proposed thermal barrier material, capable of withstanding a surface temperature of 2000 K and a temperature gradient of 1000 K across a cross section less than 10 mm. Functionally graded aluminium matrix composites reinforced with SiC particles are attractive materials for a broad range of engineering applications: the automotive, aircraft, sports, aerospace, rotors, turbines, pumps, compressors, flywheels, braking systems of automotive, railway and aerospace, and computer disc drives. All these engineering applications are usually operated at high thermal gradient and higher angular speed which may cause an increasing deformation of the disc. Therefore, a number of functionally graded materials with property of superior heat resistance have been developed.

Pandey et al., /1/, studied the steady-state creep behaviour of Al-SiCp composites under uniaxial loading conditions in the temperature range between 623 K and 723 K for different combinations of particle size and volume fraction of reinforcement, and has found that the composite with finer particle size has better creep resistance than that containing coarser ones.

Durodola and Attia, /2/, investigated the potential benefits of using several forms of fibre gradation in FGM rotating

#### Ključne reči

- modeliranje
- puzanje
- rotacioni disk od funkcionalnih kompozita
- kompozitni materijali

#### Izvod

*Puzanje kod rotacionog diska od izotropnog kompozitnog materijala sa promenljivim sadržajem čestica SiC u radijalnom pravcu je istraženo u prisustvu gradijenata temperature takođe u radijalnom pravcu. Gradijent temperature diska je posledica efekta kočenja, analizirano metodom konačnih elemenata. Puzanje je opisano Nortonovim zakonom. Rezultati pokazuju da ravnomerne brzine puzanja u većoj meri opadaju u prisustvu linearnog gradijenta čestica i/ili temperature, u poređenju sa diskom od kompozitnog materijala sa istim prosečnim sadržajem čestica uniformno raspoređenih, u izotermalnim uslovima rada.*

discs using finite element method and direct numerical integration. It was observed that the different forms of property gradation modify the stress and displacement fields in FGM discs compared with uniformly reinforced discs.

Singh and Ray, /3, 4/, have studied creep in rotating discs of composite materials. The authors in /3/ have estimated steady state creep response in a rotating isotropic FGM disc without thermal gradient using Norton's power law. It is concluded that, in a rotating isotropic FGM disc with linearly decreasing particle content from the inner to the outer radius, the steady state creep response in terms of strain rates is significantly superior compared to that in a disc with the same total particle content distributed uniformly.

Gupta et al., /5/, have analysed the creep behaviour of a rotating disc having constant thickness and made of isotropic functionally graded material (FGM).

Zenkour et al., /6/, developed an analytical solution for elastic deformation of the rotating functionally graded metal-ceramic annular disc, and obtained the closed form solution by taking into account the rigid casing condition.

#### DISTRIBUTION OF DISPERSOIDS AND CREEP CONSTANTS

Let us consider a functionally graded annular disc of inner radius  $a$  and outer radius  $b$ . The distribution of silicon carbide particles has been assumed to be linear from inner to outer radius; therefore, the density and the creep constants

will vary with radial distance. The material properties of the annular disc are assumed to be functions of the volume fraction of the constituent materials. The composition variation in terms of volume percent of silicon carbide, along the radial distance,  $V(r)$ , is given as:

$$V(r) = V_{\max} - \frac{r-a}{b-a}(V_{\max} - V_{\min}) \quad (1)$$

$$V(r) = A - Br, \quad a \leq r \leq b$$

where

$$A = V_{\max} + aB \quad \text{and} \quad (2)$$

$$B = \frac{V_{\max} - V_{\min}}{b^2 - a^2}. \quad (3)$$

Here  $V_{\max}$  and  $V_{\min}$ , are the maximum and minimum particle contents, respectively, at the inner and outer radii.

Now, using the law of mixtures, one may express the density variation  $\rho(r)$  in the composite as,

$$\rho(r) = \rho_m + (\rho_d - \rho_m) \frac{V(r)}{100}$$

where  $\rho_m$  and  $\rho_d$  are the densities of the matrix alloy and of the dispersed silicon carbide particles, respectively. Now putting the value of  $V(r)$  from Eq.(1) above gives

$$\rho(r) = \rho_m + (\rho_d - \rho_m) \frac{A - Br}{100} = A_1 - B_1 r$$

where:  $A_1 = \rho_m + (\rho_d - \rho_m) \frac{A}{100}$ ; and  $B_1 = (\rho_d - \rho_m) \frac{B}{100}$ .

If the average particle content in the FGM disc is  $V_{avg}$ , and  $t$  is the thickness of the disc, then

$$V_{avg} = \frac{\int_a^b 2\pi r t V(r) dr}{t(b^2 - a^2)\pi}. \quad (4)$$

Putting the expression of  $V(r)$  from Eq.(1) into Eq.(4), one may obtain the relation

$$V_{\min} = \frac{3V_{avg}(1 - \alpha^2)(1 - \alpha) - V_{\max}(1 - 3\alpha^2 + 2\alpha^3)}{2 - 3\alpha + \alpha^3} \quad (5)$$

where:  $\alpha = a/b$ .

The steady-state creep response of the Al-SiCp composite of varying composition using Norton's law is as follows:

$$\dot{\varepsilon}(r) = B(r) \bar{\sigma}^{n(r)} \quad (6)$$

where:  $\dot{\varepsilon}$  and  $\bar{\sigma}$  be the steady state strain rate and effective stress under bi-axial stress at a radial distance  $r$  in FGM disc. The terms  $B(r)$  and  $n(r)$  are the creep parameters for the material at radial distance  $r$  in FGM disc.

The value of  $B$  and  $n$  in terms of material variables have been extracted by using Norton's law to describe the creep results obtained by Pandey et. al., /1/, in 6061Al-SiCp composites under uniaxial loading using the following regression equations:

$$\log(B(r)) = -29 + 1729.38 \log(e) - 274.71 \log(T) - 1.98 \log(P) - 15.88 \log(V(r)) \quad (7)$$

$$\log(n(r)) = 21.54 \log(e) + 3.80 \log(T) + 0.07 \log(P) + 0.07 \log(V(r)) \quad (8)$$

## FINITE ELEMENT ANALYSIS OF THERMAL GRADIENT IN A COMPOSITE DISC

The temperature gradient originating due to the braking action of the FGM discs has been obtained by Finite Element Analysis (FEA). For this purpose, the disc with inner radius of 31.75 mm, outer radius 152.4 mm and thickness 5 mm is supposed. The FGM disc is assumed to rotate with an initial rpm of 15 600, which is reduced to 15 000 rpm due to braking action. An estimated heat flux of 130 kW/m<sup>2</sup> has been applied over an annular area with inner radius 142.4 mm and outer radius 152.4 mm, while the remaining surfaces of the FGM disc have been exposed to ambient conditions with convective heat transfer coefficient of 25 kW/m<sup>2</sup> and an ambient temperature of 303 K. For a particular ring, the thermal conductivity  $K(r)$  is assumed to be constant and calculated using the rule of mixture as given below

$$K(r) = \frac{[100 - V(r)]K_m + V(r)K_d}{100} \quad (9)$$

where the matrix conductivity is  $K_m = 247$  W/mK and the dispersoid conductivity is  $K_d = 100$  W/mK. The finite element analysis has been carried out for FGM discs having linearly decreasing particle content given by Eq.(1) with  $V_{\max}$  varying between 25 and 40 vol. % at the inner radius of the disc, while keeping the same average particle content of 20 vol. %. A similar analysis has also been conducted for the non-FGM disc having a same particle distribution of 20 vol. %. The temperature  $T$ , obtained at any radius  $r$  is presented below in the form of regression equation as

$$T(r) = a_0 + a_1 r + a_2 r^2 + a_3 r^3 + a_4 r^4 + a_5 r^5 \quad (10)$$

where the coefficients  $a_1, a_2, a_3, a_4$ , and  $a_5$  for a different disc are taken from Gupta et al., /4/.

## MATHEMATICAL FORMULATION

Consider an aluminium silicon-carbide particulate composite disc of constant thickness  $h$  having inner radius  $a$ , and outer radius  $b$ , rotating with angular velocity  $\omega$  (rad/s). From symmetry considerations, principal stresses are in the radial, tangential and axial directions. For the purpose of analysis, the following assumptions are made:

- stresses at radius of the disc remain constant with time i.e. steady state condition of stress is assumed,
- elastic deformations are small for the disc and can be neglected as compared to the creep deformations,
- biaxial state of stress ( $\sigma_z = 0$ ) exists at any point of the disc,
- frictional shear stress induced due to braking action is estimated to be  $10^{-5}$  MPa, which is very small compared to creep stresses and therefore, can be neglected,
- the composite shows a steady state creep behaviour which may be described by Norton's law as given by Eq.(6).

The generalized constitutive equations for creep in the FGM disc have the form, /3/,

$$\dot{\varepsilon}_r = \frac{\dot{\varepsilon}}{2\bar{\sigma}} [2\sigma_r - (\sigma_\theta + \sigma_z)] \quad (11)$$

$$\dot{\varepsilon}_\theta = \frac{\dot{\varepsilon}}{2\bar{\sigma}} [2\sigma_\theta - (\sigma_z + \sigma_r)] \quad (12)$$

$$\dot{\epsilon}_z = \frac{\dot{\bar{\epsilon}}}{2\bar{\sigma}} [2\sigma_z - (\sigma_r + \sigma_\theta)] \quad (13)$$

where the effective stress  $\bar{\sigma}$  is given by

$$\bar{\sigma} = \frac{1}{\sqrt{2}} [(\sigma_\theta - \sigma_r)^2 + (\sigma_r - \sigma_z)^2 + (\sigma_z - \sigma_\theta)^2]^{1/2} \quad (14)$$

where  $\dot{\epsilon}_r, \dot{\epsilon}_\theta, \dot{\epsilon}_z$  and  $\sigma_r, \sigma_\theta, \sigma_z$  are the strain rates and stresses respectively in the directions indicated by the subscripts and  $\dot{\bar{\epsilon}}$  is the effective strain rate. For biaxial state of stress  $(\sigma_r, \sigma_\theta)$ ,

$$\bar{\sigma} = \frac{1}{\sqrt{2}} [\sigma_\theta^2 + \sigma_r^2 + (\sigma_r - \sigma_\theta)^2]^{1/2}. \quad (15)$$

Equations from (6) and (15) yield

$$\dot{\epsilon}_r = \frac{d\dot{u}_r}{dr} = \frac{B(r)\sigma_\theta^{n(r)} [2(x(r))^2 - 2x(r) + 2]^{(n(r)-1)/2} [2x(r)-1]}{2^{(n(r)+1)/2}} \quad (16)$$

$$\dot{\epsilon}_\theta = \frac{\dot{u}_r}{r} = \frac{B(r)\sigma_\theta^{n(r)} [2(x(r))^2 - 2x(r) + 2]^{(n(r)-1)/2} [2-x(r)]}{2^{(n(r)+1)/2}} \quad (17)$$

$$\dot{\epsilon}_z = -(\dot{\epsilon}_r + \dot{\epsilon}_\theta) \quad (18)$$

where  $x(r) = \sigma_r/\sigma_\theta$  is the ratio of radial and tangential stress at any radius  $r$ .

Dividing Eq.(16) by Eq.(17):

$$\varphi(r) = \frac{2x(r)-1}{1-x(r)}. \quad (19)$$

The equation of equilibrium for a rotating disc can be written as:

$$\frac{d}{dr}(r\sigma_r) - \sigma_\theta + \frac{\rho(r)\omega^2 r^2}{g} = 0 \quad (20)$$

The boundary conditions are

$$\sigma_r(a) = 0 = \sigma_r(b). \quad (21)$$

Equations (16), (17), (20) and (21) can be solved to obtain  $\sigma_\theta(r)$  as given below

$$\sigma_\theta(r) = \frac{(b-a)\sigma_{\theta_{avg}}}{\int_a^b \psi(r) dr} \psi(r) \quad (22)$$

where

$$\psi(r) = \frac{2^{(n(r)+1)/2} \exp\left\{\int_a^r \frac{\varphi(r)}{r} dr\right\}}{\left[2(x(r))^2 - 2x(r) + 2\right]^{(n(r)-1)/2} [2-x(r)]} \quad (23)$$

and

$$\sigma_{\theta_{avg}} = \frac{1}{b-a} \int_a^b \sigma_\theta dr. \quad (24)$$

Now  $\sigma_r(r)$  can be obtained by integrating from  $a$  to  $r$  as

$$\sigma_r(r) = \frac{1}{r} \int_a^r \sigma_\theta(r) dr - \frac{\omega^2}{gr} \left[ A_1 \frac{r^3 - a^3}{3} - B_1 \frac{r^4 - a^4}{4} \right] \quad (25)$$

As the tangential stress  $\sigma_\theta$  and the radial stress  $\sigma_r$  are determined by Eqs.(22) and (25) at any point within the composite disc, the strain rates  $\dot{\epsilon}_r$  and  $\dot{\epsilon}_\theta$  are calculated from Eqs.(16) and (17), respectively.

### NUMERICAL COMPUTATION

The stress distribution is evaluated from the above analysis by iterative numerical scheme of computation. For rapid convergence, 75% of the value of  $\sigma_\theta(r)$  obtained in the current iteration has been mixed with 25% of the value of  $\sigma_\theta(r)$  obtained in the last iteration for the use in the next iteration.

### RESULTS AND DISCUSSION

A computer program based on the analysis presented is developed and results obtained are validated with the experimental results by Wahl et. al., /7/, for the same type of disc. This comparison is shown in Fig. 1. It is observed from this figure that there is good agreement between the results obtained from the present analysis. The tangential stress in the FGM disc-1 operating under a thermal gradient is higher near the inner radius, and lower near the outer radius, as compared to disc-2 and disc-3 as shown in Fig. 2. The non-FGM disc-4 without particle or thermal gradient shows a relatively uniform distribution of tangential stress. These changes in the tangential stress are due to different temperature gradients as well as changed density due to different particle contents near inner and outer radii as compared to the non-FGM disc. The effect of thermal gradient on the tangential stress as observed in the non-FGM discs, disc-3 and disc-4, is similar to that in FGM discs, disc-1 and disc-2.

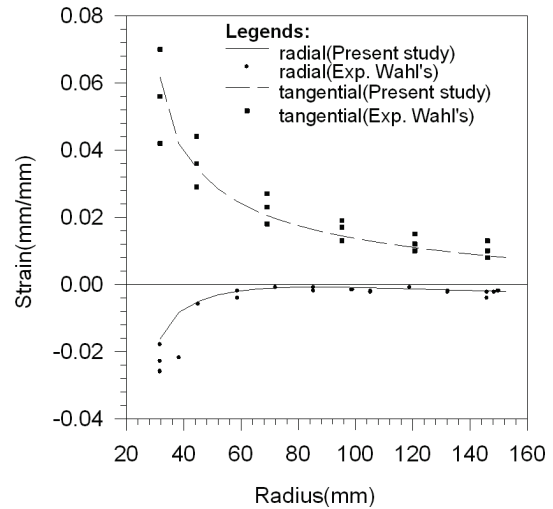


Figure 1. Comparison of theoretical (present study) and experimental strains in a rotating steel disc.

The radial stress in disc-1 is higher over the entire radius as compared to any discs as shown in Fig. 3. The effect of imposing any type of gradient separately or simultaneously is similar to that in tangential stress.

In Fig. 4, the tangential strain rate decreases significantly over the entire radius in the FGM disc-1 operating under the thermal gradient developed, compared to any of the other discs operating under conditions as given in /4/. Although the tangential stress in the FGM disc-1 is higher near the inner radius than the FGM disc-2, as shown in Fig. 2, but the lower operating temperature near the inner radius of the FGM disc-1 is able to reduce the creep rate overcoming the effect of higher stress. Clearly, the temperature near the inner radius and the tangential stress near the outer radius of the FGM disc-1

dominate the creep behaviour when compared to those observed in the FGM disc-2 under isothermal condition.

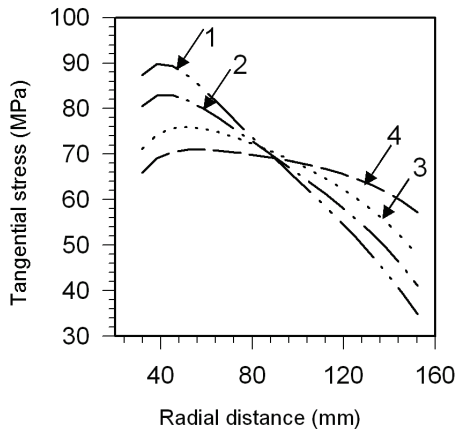


Figure 2. Variation of tangential stress along radial distance in FGM and non-FGM disc with/without particle/thermal gradient.

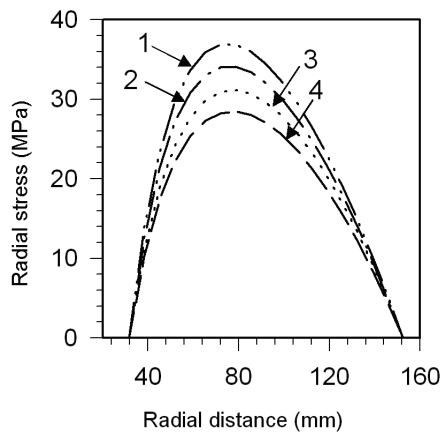


Figure 3. Variation of radial stress along radial distance in FGM and non-FGM disc with/without particle/thermal gradient.

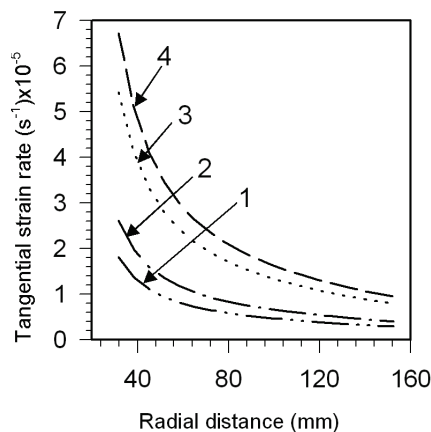


Figure 4. Variation of tangential strain rate along radial distance in FGM and non-FGM disc with/without particle/thermal gradient.

The tangential strain rate in the non-FGM disc-3 with thermal gradient alone is higher than the observed in the FGM disc-1 and FGM disc-2, since both discs have the advantage of particle gradient and the FGM disc-1 has the reinforcing advantage of thermal gradient as well. The FGM disc-4, which has neither the thermal gradient nor particle gradient, displays the highest tangential creep rate observed in this study, as shown in Fig. 4.

In Fig. 5, the effect of imposing both particle gradient and thermal gradient on the radial strain rate is also similar to that observed for tangential strain rate.

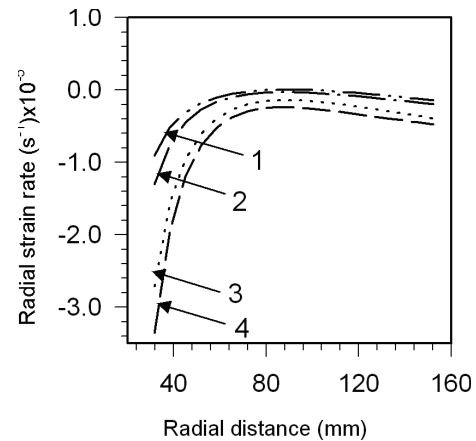


Figure 5. Variation of radial strain rate along radial distance in FGM and non-FGM disc with/without particle/thermal gradient.

## CONCLUSIONS

Based on the results and discussion presented in this paper, the following main conclusions may be drawn.

The creep response of the functionally graded disc with particle and/or thermal gradient is superior to a disc without any type of gradient.

The creep strain can be controlled by choosing appropriate particle/thermal gradient.

Since particle/thermal gradient plays a significant role in developing the creep strains, it may be taken care of while designing a rotating disc.

## REFERENCES

- Pandey, A.B., Misra, R.S., Mahajan, Y.R. (1992), *Steady state creep behaviour of silicon carbide particulate reinforced aluminium composites*, Acta Metal. Mater., 40(8): 2045-2052.
- Durodola, J.F., Attia, O. (2000), *Deformation and stresses in functionally graded rotating disks*, Comp. Sci. & Tech., 60(7): 987-995.
- Singh, S.B., Ray, S. (2001), *Steady-state creep behavior in an isotropic functionally graded material rotating disc of Al-SiC composite*, Metall. Mater. Trans. A, 32(7): 1679-1685.
- Singh, S.B. (2008), *One parameter model for creep in a whisker reinforced anisotropic rotating disc of Al-SiCw composite*, Europ. J Mech. A/Solids, 27(4), 680-690.
- Gupta, V.K., Singh, S.B., Chandrawat, H.N., Ray, S. (2005), *Creep in an isotropic rotating disc of Al-SiCp composites*, Ind. J Pure & Appl. Math., 34(12): 1797-1807.
- Zenkour, A.M. (2007), *Elastic deformation of the rotating functionally graded annular disk with rigid casing*, J Mat. Sci., 42 (23): 9717-9724.
- Wahl, A.M., Sankey, G.O., Manjoine, M.J., Shoemaker, E. (1954), *Creep tests of rotating disks at elevated temperature and comparison with theory*, J Appl. Mech., 21(3): 225-235.